Raman Imaging: Defining the Spatial Resolution of the Technology

Chemical images of polystyrene beads on silicon acquired using Raman mapping and image processing are reviewed. The effects of the objective on the quality of the final image, particularly its magnification and numerical aperture, and the step size of the map, are discussed as well.

Fran Adar, Eunah Lee, Sergey Mamedov, and Andrew Whitley

Raman images constructed from hyperspectral cubes recorded under well-defined confocal conditions show high-quality chemical contrast. Careful studies are required to determine the optimum measurement conditions and limiting spatial resolution of the technique. Calculations and measurements of the laser spot size for the high numerical aperture (n.a.) objectives indicate that spatial resolution of a wavelength ($\leqslant$ 0.5 μm) is achievable under good conditions. What does that mean in terms of the quality of a Raman image?

Preliminary measurements have been made on polystyrene microspheres of the order of 8 μm in diameter, dispersed on silicon. The spectrum from the center of one of the beads is shown in Figure 1. The silicon substrate has a sharp band at 520 cm^{-1} from the first-order phonon, and a broad second-order feature between 935 and 1010 cm^{-1}. All the other sharp bands in the spectrum are attributed to polystyrene. The intensity of the strong band near 1000 cm^{-1} is used to construct the Raman images shown later.

Raman chemical images of one of these beads are shown in Figure 2. The bead is color-coded red and the substrate is color-coded green. The same 100x objective was used to make the maps, but the increment between data points was varied from 1 μm, to 0.5 μm, and to 0.1 μm. Inspection of these images indicates a startling improvement in the image quality when decreasing the increment between data points. The implication of this result is that even if the

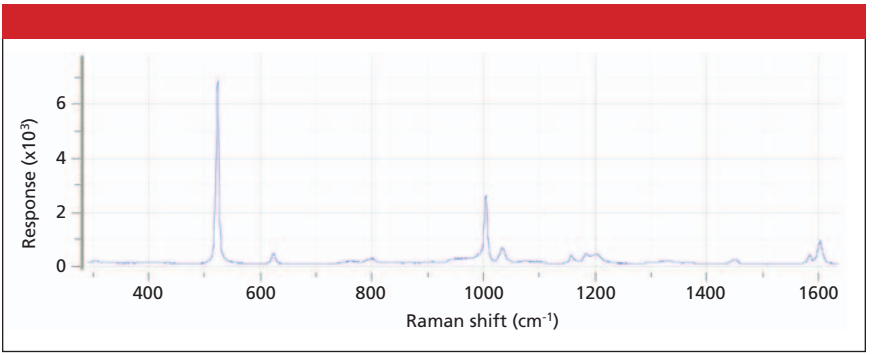

Figure 1: Raman spectrum recorded with the 100x objective from the center of an 8-μm bead on a (001) Si substrate.

"resolution" of the technique is somewhere between 0.5 and 1 μm, the best information can be extracted by mapping with data increments considerably smaller than this.

These micrographs have the silicon and polystyrene intensities superimposed. What is curious is the "hot spots" on the sides of the spheres. What we have noticed is that rather than the sphere shadowing the silicon intensity, the presence of the sphere in fact intensifies it, presumably because of the focusing properties of the sphere. To explore this phenomenon, an *xz* profile was recorded and is shown in Figure 3. Again, the red color represents the polystyrene bead and the green represents the silicon. If there were simple shadowing, the silicon signal would be most intense to the sides of the sphere, and there would be little intensity above the sphere. Because significant silicon intensity is observed above the sphere, at heights where the silicon intensity is quite low if there is no sphere, we must assume that the presence of the sphere is acting to refocus the laser and return more silicon intensity than expected.

The second set of measurements were made with polystyrene spheres of uniform dimension, dispersed from solution also on a silicon substrate. Monodispersed polymer beads make ideal samples for this type of test. When deposited from aqueous solutions onto a silicon substrate, it is possible to find isolated spheres, small clusters, and close-packed films. In line with the results and conclusion of the measurement shown earlier, and from our previous report (1), the maps from these spheres were recorded with intervals considerably smaller than the expected spatial resolution.

Using polystyrene microspheres of sizes of 5.2 μm, Raman images were generated with objectives 100x/n.a. = 0.9, 50x/n.a. = 0.75, and 20x/n.a. = 0.4. By using objectives with different magnifications and numerical apertures, it is possible to explore the predicted role of the numerical aperture on the properties of the Raman chemical image.

The Raman images were acquired on the Aramis using a 1200 g/mm grating, the 532-nm laser (approximately 10 mW at the sample after the

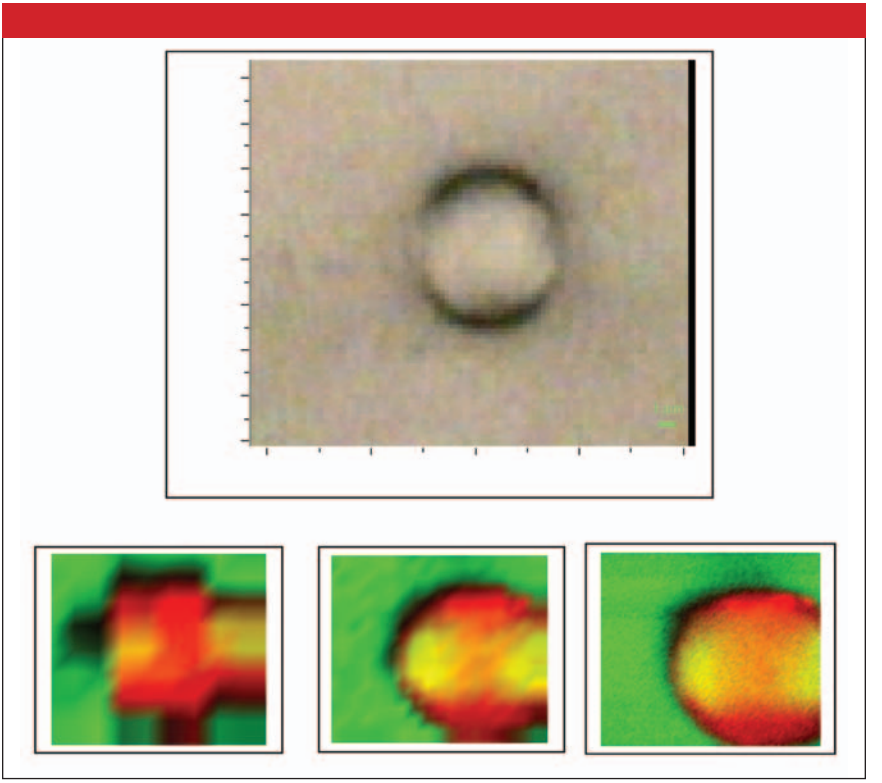

Figure 2: Optical micrograph (top) and Raman chemical image of an 8-μm polystyrene bead recorded with 1.0, 0.5, and 0.1 μm/d.

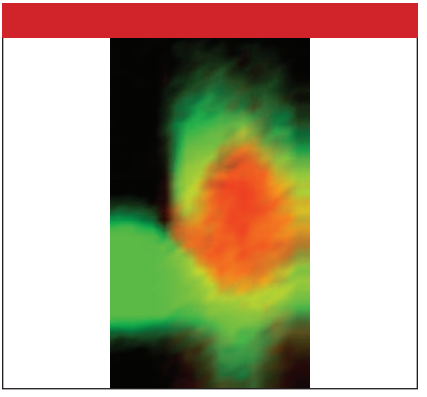

Figure 3: XZ Raman chemical map of 8-μm bead on silicon. The range of the map was 20 μm in the Z direction, and 9 μm in the X direction. The presence of the silicon signal (green) above and below the polystyrene sphere (red) suggests that the sphere is acting as a focusing element.

OD 0.6 neutral density filter), slit and confocal hole sizes of 100 and 400 μm, respectively. The motorized *xy* stage was incremented by 0.2 μm per data point. This value is considerably smaller than the nominal spot size — of the order of a wavelength of the light. The images were collected with two 1-s integrations, which enables the cosmic ray removal routine.

Figure 4 shows optical micrographs of the beads taken first with the 20x objective, and then with the 50x; this latter micrograph is shown full scale and is then zoomed to the region of interest. Maps of this region were acquired with the 100x,

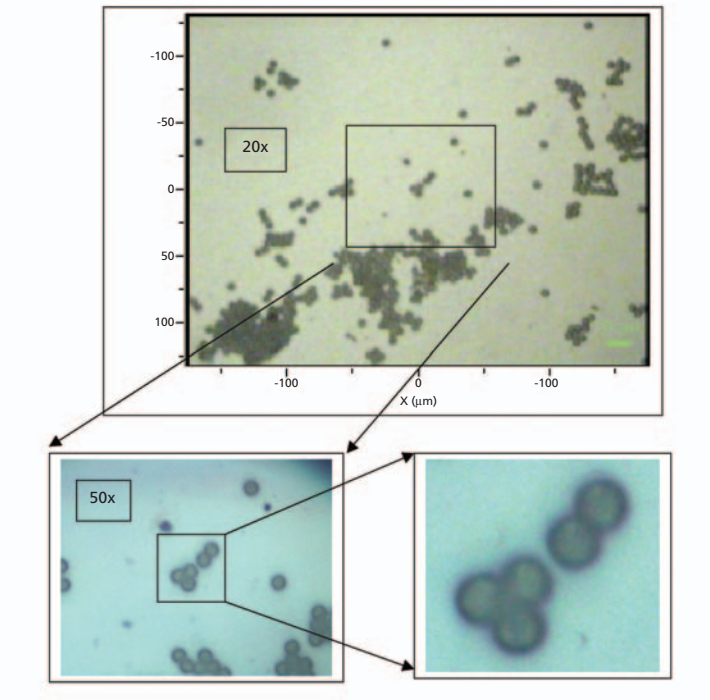

Figure 4: Optical micrograph of a dispersion of 5.2-µm spheres of polystyrene dispersed on silicon. The top micrograph was recorded with the 20x objective, and the lower left figure was recorded with the 50x objective. The micrograph on the lower right was extracted from the figure to its left.

50x, and 20x objectives. In this region, there are two clusters: one with three beads and one with two.

Figure 5 shows the Raman maps recorded with the three objectives. We emphasize again that all conditions were the same except for the magnification and numerical aperture of the objectives. Therefore any differences in the Raman maps can be attributed to the characteristics of the objective. Clearly the 100x, with the largest numerical aperture, provides the best quality image, with the 50x not far behind — a fact that is not too surprising since the numerical apertures are so close (0.9 versus 0.75). To more quantitatively characterize the quality of these images, line profiles were extracted through the two-sphere cluster on the upper right. Those line profiles are reproduced in the final figure, and reinforce the conclusion that the quality of the Raman chemical images is directly correlated with the numerical aperture of the objective used to create the image.

Figure 6 shows profiles extracted from the three images in lines across the two spheres in the upper right part of the field. The dip in intensity at the midpoint is an indication of the resolution of the image. Again,

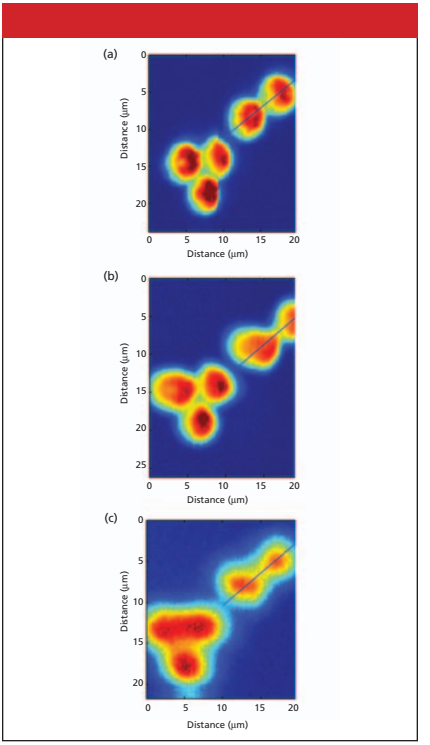

Figure 5: Raman chemical maps of 5.18-µm spheres of polystyrene recorded with 100x, 50x, and 20x objectives. Increments between data points were 0.2 µm for all three images. The diagonal lines across the pair of spheres in the upper right part of the images represent the locus of points used for the line profiles shown in Figure 6.

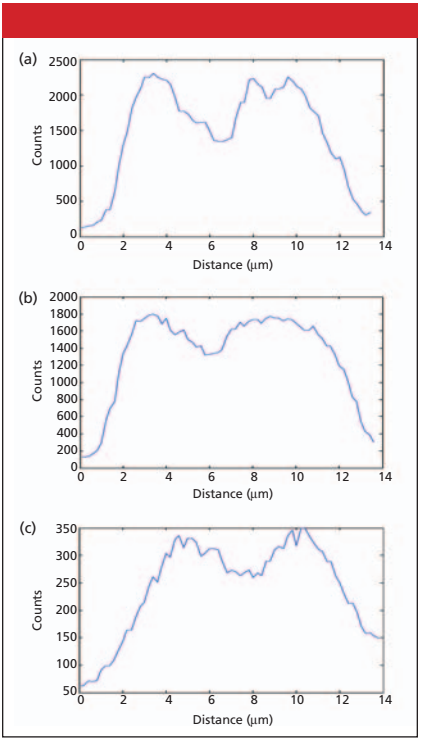

Figure 6: Line profiles across the two contiguous spheres.

the higher the numerical aperture of the objective used, the better the definition of this dip.

Conclusions

The results of this study and our previous report (1) show that the use of the highest numerical aperture objective coupled with a step size 5–10 times smaller than the laser spot size will provide the highest quality chemical images. This is of particular relevance and importance for Raman imaging of biological material such as bacteria and subcellular organelles, where the features of interest push the spatial resolution of the technique to its limit. The introduction of faster detectors, advanced spectral imaging software, and new mapping stages capable of stepping with nanometric precision and reproducibility has taken Raman imaging to a new level of capability useful to both spectroscopists and microscopists alike.

References

(1) E. Lee, F. Adar, and A. Whitley, *The Application Notebook*, *Spectroscopy,* March 2006, p. 21.

Fran Adar, Eunah Lee, Sergey Mamedov, and **Andrew Whitley** are with Horiba Jobin Yvon, Inc., Edison, New Jersey. ■